MBN Research Center

Horizon Europe EIC-Pathfinder Project TECHNO-CLS: "Emerging technologies for crystal-based gamma-ray light sources"

A.V. Solov'yov

MBN Research Center, Frankfurt am Main, Germany

www.mbnresearch.com

Annual Workshop of Horizon Europe EIC-Pathfinder Project TECHNO-CLS,
Ferrara, Italy, October 5-6, 2023

Outline

MBN Research Center

- **Introduction**
  - Horizon Europe EIC-Pathfinder Project TECHNO-CLS
  - Oriented Crystal based Light Sources (CLS)
  - CLS related technologies
- **MBN Explorer and MBN Studio 5.0: capabilities and TECHNO-CLS related case studies**
  - MBN Explorer and MBN Studio software packages: capabilities and TECHNO-CLS related case studies
  - Characterization of CLSs
- **Concluding remarks**

Horizon Europe EIC-PATHFINDER TECHNO-CLS project : *Emerging technologies for crystal-based gamma-ray light sources (2022-2027)*

MBN Research Center

TECHNO-CLS

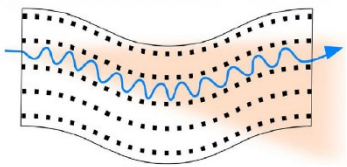

MBN Research Center

INFN
Istituto Nazionale di Fisica Nucleare

Università degli Studi di Ferrara
- EX LABORE FRUCTUS -

Johannes Gutenberg Universität Mainz

JG|U

ESRF

Associated partners:

1. FiZ- Frankfurter Innovationszentrum

2. E6-Elementsix

University of Kent

Università degli Studi di Padova

Hellenic Mediterranean University

Funded by the European Union

Project 101046458 — TECHNO-CLS

Horizon Europe EIC-PATHFINDER TECHNO-CLS project continues research conducted within **FP6-PECU, FP7-CUTE, H2020-PEARL and H2020 N-LIGHT** projects.

Oriented crystal based light sources

MBN Research Center

Selected examples of the novel Crystal based Light Sources (CLSs). Black circles and lines mark atoms of crystallographic planes, wavy curves show trajectories of the channeling particles, shadowed areas refer to radiation.

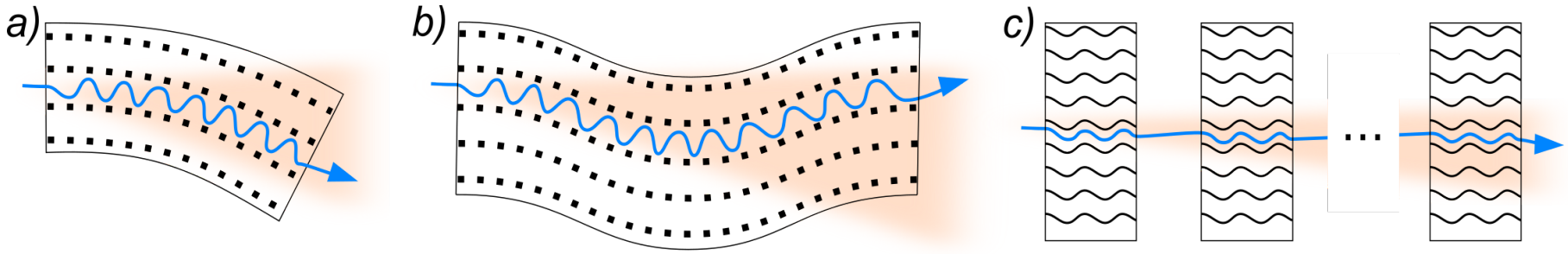

Figure from A.V. Korol, and A.V. Solov'yov, Eur. Phys. J. D (2020) 74: 201

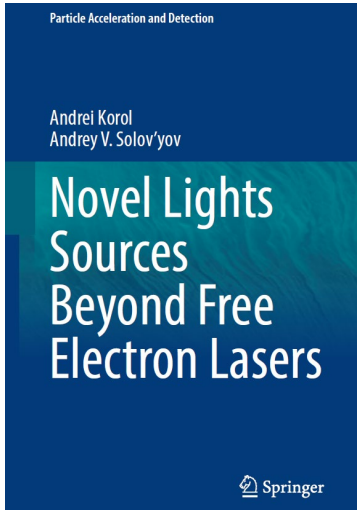

- A.V. Korol, A.V.Solov'yov, *Novel Lights Sources Beyond Free Electron Lasers*, Particle Acceleration and Detection series, Springer Nature Switzerland, Cham (2022)
- A.V. Korol and A.V. Solov'yov, *Crystal-based intensive gamma-ray light sources* (Topical Review), Eur. Phys. J. D, vol. 74, 201 (2020)
- A.V. Korol, G.B. Sushko, and A.V. Solov'yov, *All-atom relativistic molecular dynamics simulations of channeling and radiation processes in oriented crystals* (Topical Review), Eur. Phys. J. D, vol. 75, 107 (2021)
- A.V. Korol, A.V. Solov'yov, Greiner, *Channeling and Radiation in Periodically Bent Crystals*, Second Edition, Springer–Verlag, Berlin, Heidelberg (2014)

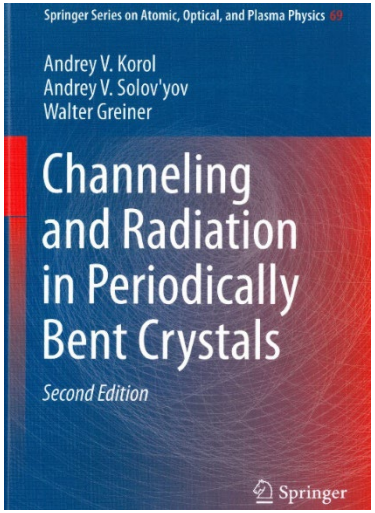

Crystalline vs magnetic undulator

MBN Research Center

Magnetic undulator:

λ_u~1 cm, $\hbar\omega$~10 keV

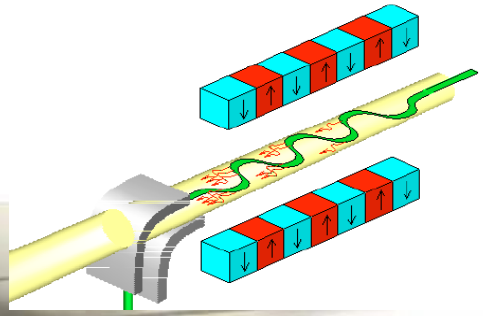

Crystalline undulator:

λ_u~10 μm, $\hbar\omega$~0.1 …10 MeV

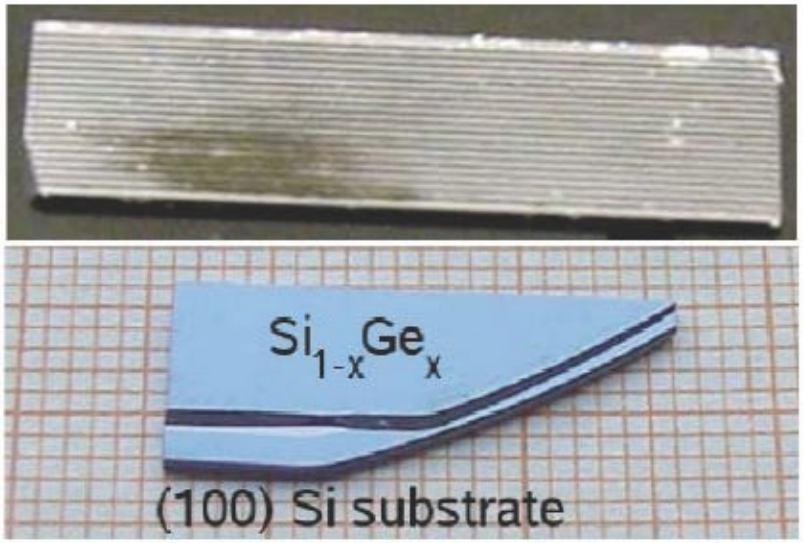

Fig. 1.3 *Left:* Magnetic undulator for the X-ray laser XFEL [179]. The picture is taken from [180]. *Right top:* laser-ablated diamond crystal. The crystal size is $4 \times 2 \times 0.3$ mm^3. The undulator period is $\lambda_u = 50\,\mu$m. The picture is taken from [74]. *Right bottom:* a $Si_{1-x}Ge_x$ superlattice crystalline undulator with four periods. Periodically varied Ge content (from $x = 0$ to $x_{max} = 0.5\%$) gives rise to the undulator period $\lambda_u = 50\,\mu$m. The picture is courtesy of J.L. Hansen, A. Nylandsted and U. Uggerhøj (University of Aarhus).

CU-LSs versus FEL and SR

MBN Research Center

Brilliance of a photon source relates the number of photons of a given energy emitted per unit time interval, unit source area, unit solid angle and per bandwidth:

$$B_n = \frac{\Delta N_{\omega_n}}{10^3 \left(\Delta\omega_n/\omega_n\right)(2\pi)^2 \varepsilon_x \varepsilon_y} \frac{I}{e}$$

- n – harmonic number
- $\omega_n, \Delta\omega_n$ – energy and width of the nth harmonic
- $\Delta\omega_n/\omega_n$ – bandwidth (=BW)
- ΔN_{ω_n} – number of photons with $\omega \in \left[\omega_n - \Delta\omega_n/2, \omega_n + \Delta\omega_n/2\right]$
- I – electric current of the beam
- $\varepsilon_{x,y}$ – emittance of the photon source along

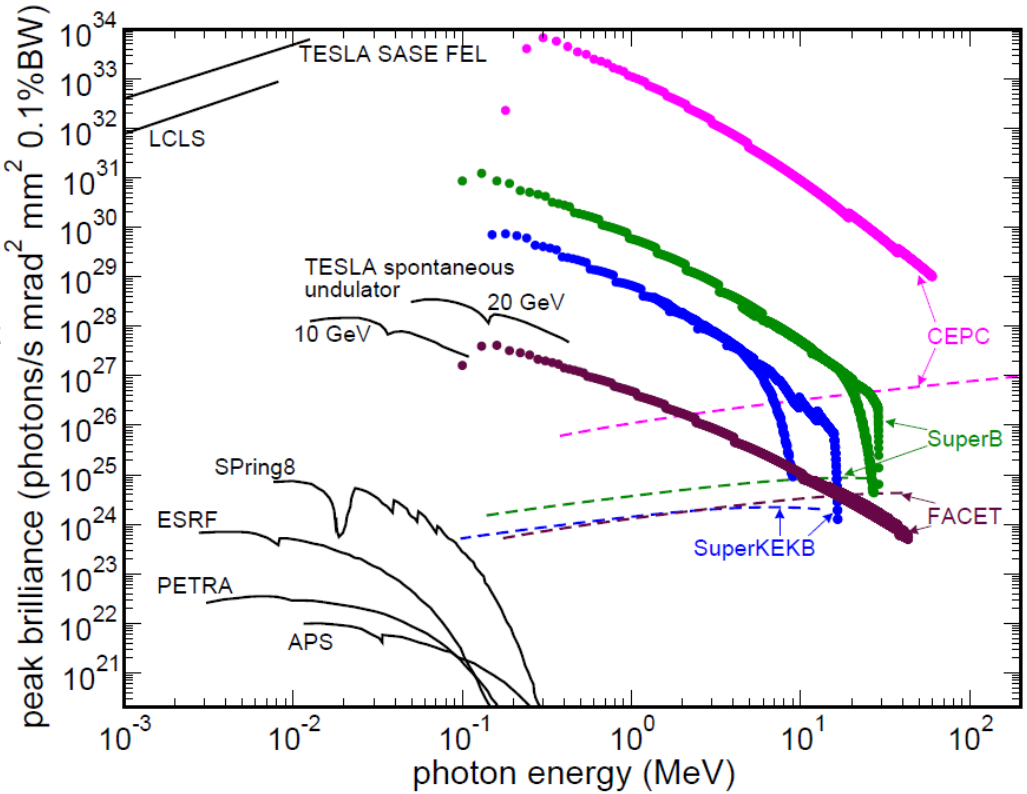

Figure 5. Peak brilliance of superradiant CUR (thick solid curves) and spontaneous CUR (dashed lines) from diamond(110) CUs calculated for the SuperKEKB, SuperB, FACET-II and CEPC positron beams versus modern synchrotrons, undulators and XFELs.

A.V Korol, A.V Solov'yov, Eur. Phys. J. D (2020) 74: 201

Photon emission by an ultra-relativistic particle

Lorentz factor: $\gamma = \dfrac{1}{\sqrt{1 - v^2/c^2}}$

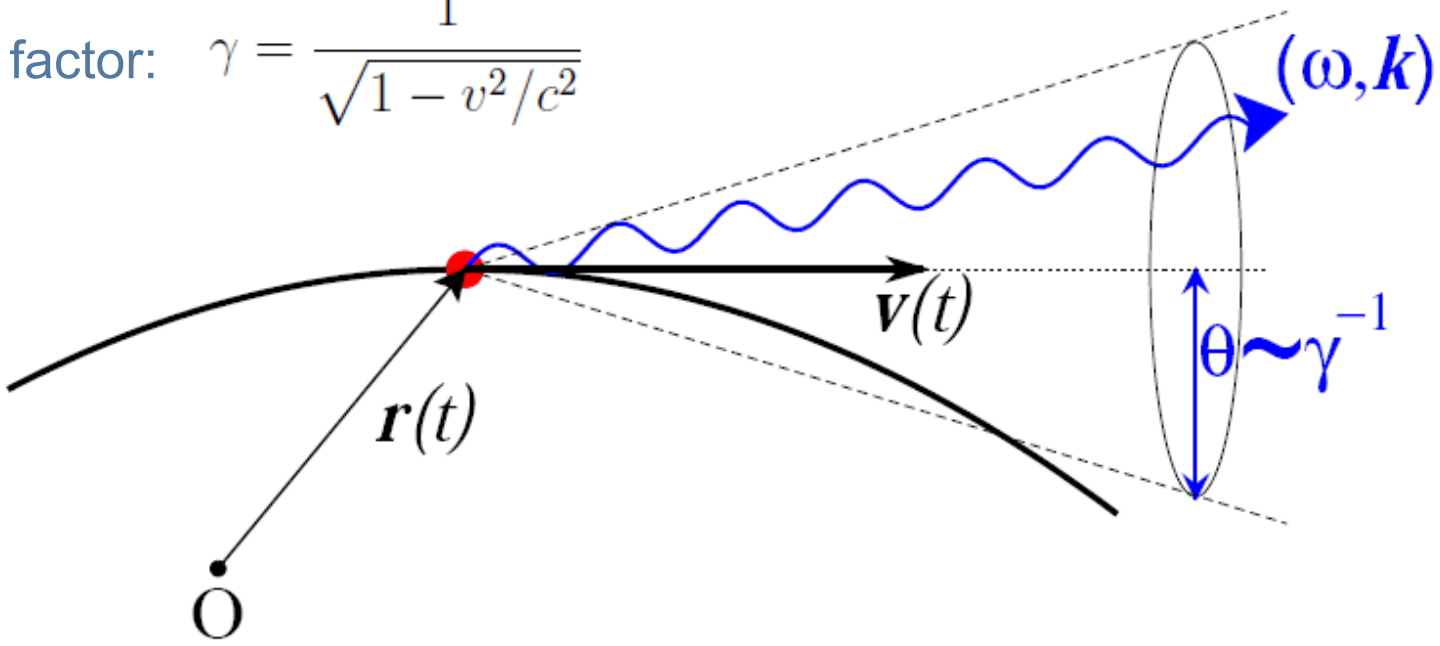

The photon emission occurs within the (narrow) cone $\theta \sim \gamma^{-1}$ along the instant velocity.

Figure from A. Korol, A. Solov'yov, W. Greiner, *Chan. and Rad. In Periodically Bent Crystals*, Springer-Verlag Berlin, Heidelberg (2013)

Radiative spectra

$$\frac{\mathrm{d}E(\theta \le \theta_0)}{\hbar\,\mathrm{d}\omega} = \frac{1}{N_0}\sum_{j=1}^{N_0}\int_0^{2\pi}\int_0^{\theta_0}\frac{\mathrm{d}^3E_j}{\hbar\,\mathrm{d}\omega\,\mathrm{d}\Omega}\,\mathrm{d}\Omega$$

θ_0 – defined by the aperture

Spectral-angular distribution for an individual trajectory

Quasiclassical formalism:

$$\frac{\mathrm{d}^3E}{\hbar\mathrm{d}\omega\,\mathrm{d}\Omega} = \alpha\frac{q^2\omega^2}{8\pi^2}\int_{-\infty}^{\infty}\mathrm{d}t_1\int_{-\infty}^{\infty}\mathrm{d}t_2\,\mathrm{e}^{\mathrm{i}\omega'(\psi(t_1)-\psi(t_2))}\left[(1+(1+u)^2)\left(\frac{\mathbf{v}_1\cdot\mathbf{v}_2}{c^2}-1\right)+\frac{u^2}{\gamma^2}\right]$$

$$\psi(t) = t - \mathbf{n}\cdot\mathbf{r}(t)/c$$

$$\omega' = (1+u)\,\omega$$

$$u = \frac{\hbar\omega}{\varepsilon - \hbar\omega}$$

Accounts for the radiative recoil (a quantum effect)

V.N. Baier, V.M. Katkov, V.M. Strakhovenko, Electromagnetic Processes at High Energies in Oriented Single Crystals. World Scientific, Singapore (1998).

Radiation from a crystalline undulator

MBN Research Center

Basic idea (Korol, Solov'yov, Greiner, J.Phys.G, v.24, L45 (1998); reviews: *International Journal of Modern Physics E*, v.8, p.49-100 (1999); v.13, p.867-916 (2004)); PRL, 98, 164801, (2007); Monograph, Second Edition, Springer–Verlag, Berlin, Heidelberg (2014)

The radiation is generated by a bunch of ultra-relativistic positrons (ε=0.5…10 GeV) channeling in a crystal along periodically bent crystallographic planes. The periodicity of trajectories results in the undulator-type radiation due to the constructive interference of the photons emitted from similar parts of the trajectory.

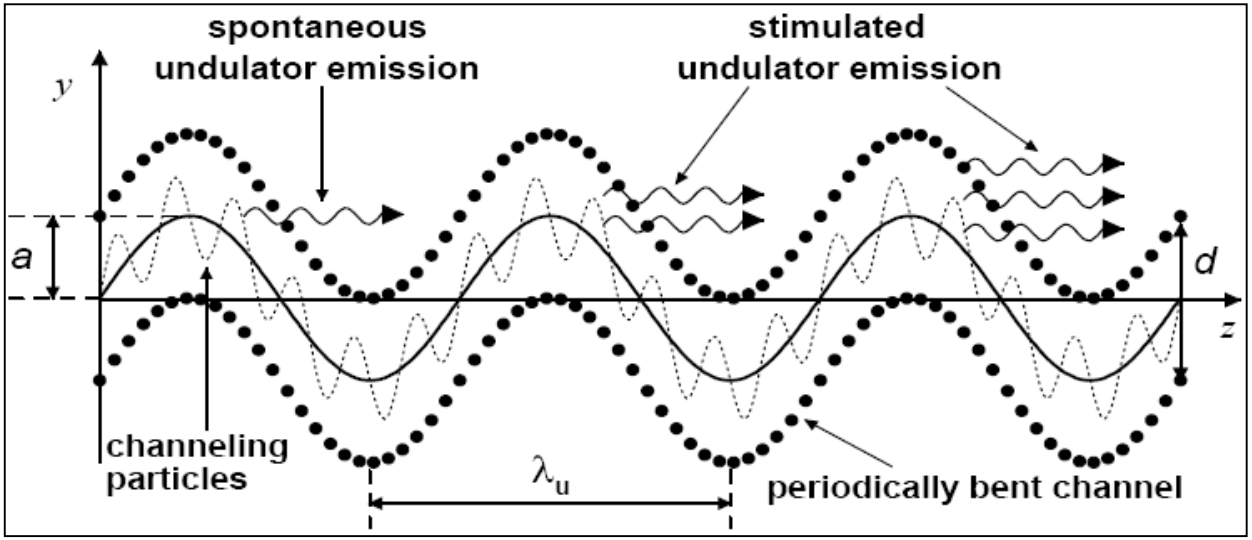

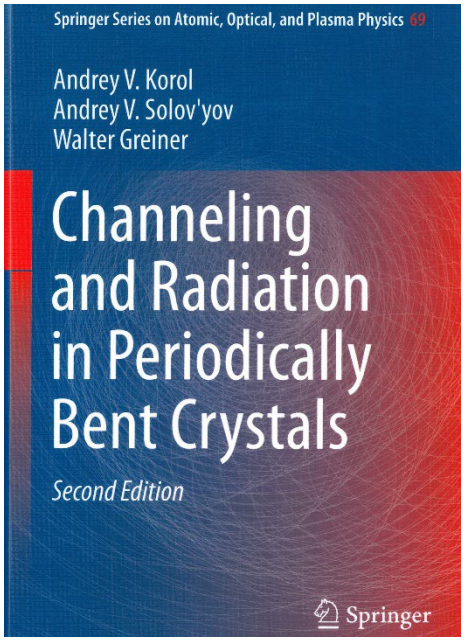

d=1…2 Å - the interplanar spacing
a=(10…50)*d* – the amplitude of bending
λ_u=(10^4…10^5)*a* – the period of bending

$d << a << \lambda$

Feasibility of a crystalline undulator

MBN Research Center

The summary of all essential conditions (Korol, Solov'yov,Greiner 1998, 2004):

$$
\begin{cases}
C = (2\pi)^2 \dfrac{\varepsilon}{qU'_{\max}} \dfrac{a}{\lambda^2} \ll 1 & \text{stable channeling} \\
d \ll a \ll \lambda & \text{large-amplitude regime} \\
N = \dfrac{L}{\lambda} \gg 1 & \text{large number of undulator periods} \\
L \leq \min\left[L_{\mathrm{d}}(C), L_a(\omega)\right] & \text{account for the dechanneling and photon attenuation} \\
\dfrac{\Delta\varepsilon}{\varepsilon} \ll 1 & \text{low radiative losses}
\end{cases}
$$

If these are met then:

- within the length *L* the particle experiences stable planar channeling
- characteristic energies of the undulator and channeling radiation are well separated
- intensity of the undulator radiation is higher than that of the channeling radiation.
- emission spectrum is stable towards the radiative losses.

CU parameter ranges

MBN Research Center

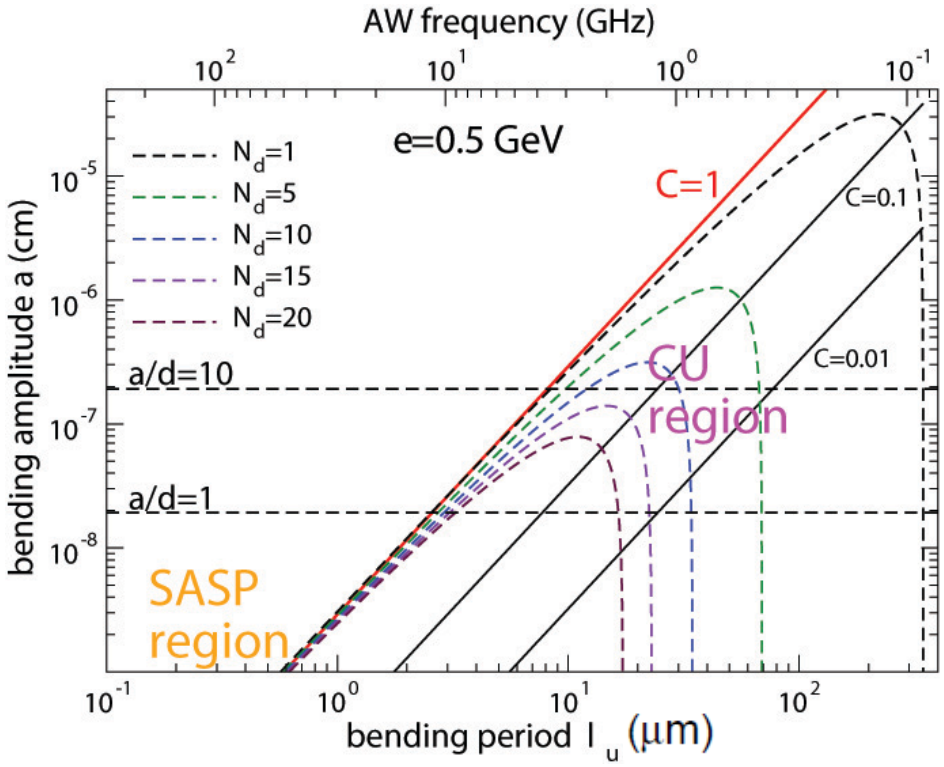

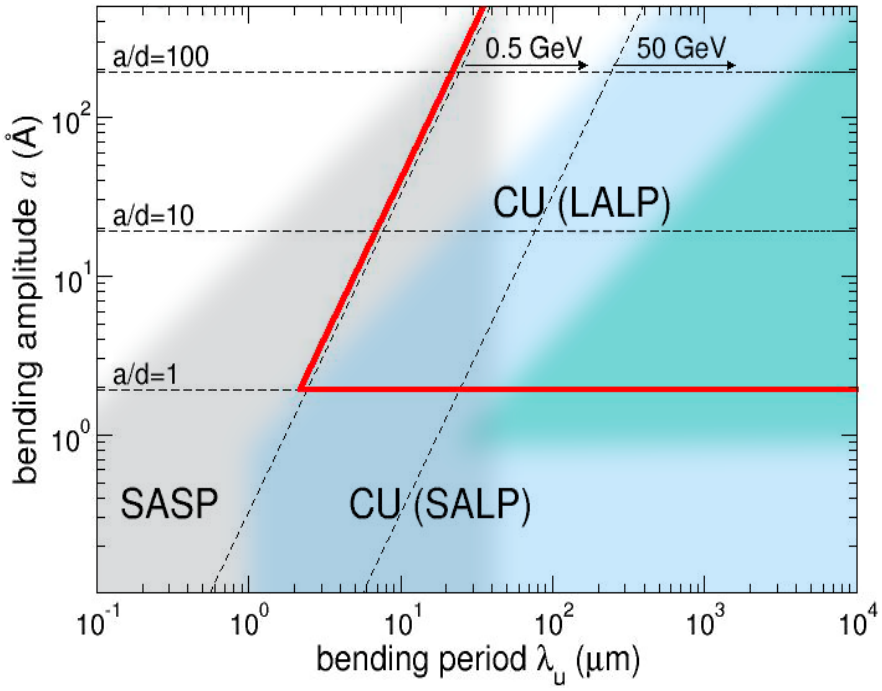

Left figure. Bending amplitude, a, vs bending period, λ, consistent with the condition C<1 and calculated for various numbers of undulator periods N_d as indicated for e=0.5 Gev ($\gamma = 10^3$) positron channeling in *Si* along (110) crystallographic plane. Bending profile $y=a\sin(2\pi z/\lambda)$.
A.Korol, W.Krause, A.Solov'yov, W.Greiner, J.Phys.G: Nucl.Part.Phys., v.26, L87-L95 (2000);
From A.Korol, A.Solov'yov, W.Greiner, Chan. and Rad. In Periodically Bent Crystals, Second Edition, Springer–Verlag, Berlin, Heidelberg (2014);
Right figure. Shadowing indicates the ranges accessible by means of modern technologies: superlattices (grey), surface deformations (green), AWs (blue); ***From Korol, Solov'yov, Eur. Phys. J. D, vol. 74, 201 (2020)***

Experimental characterisation of PBCs

MBN Research Center

- X-ray diffraction at the ID11 beamline of ESRF ($Si_{(1-x)}$ Ge_x)

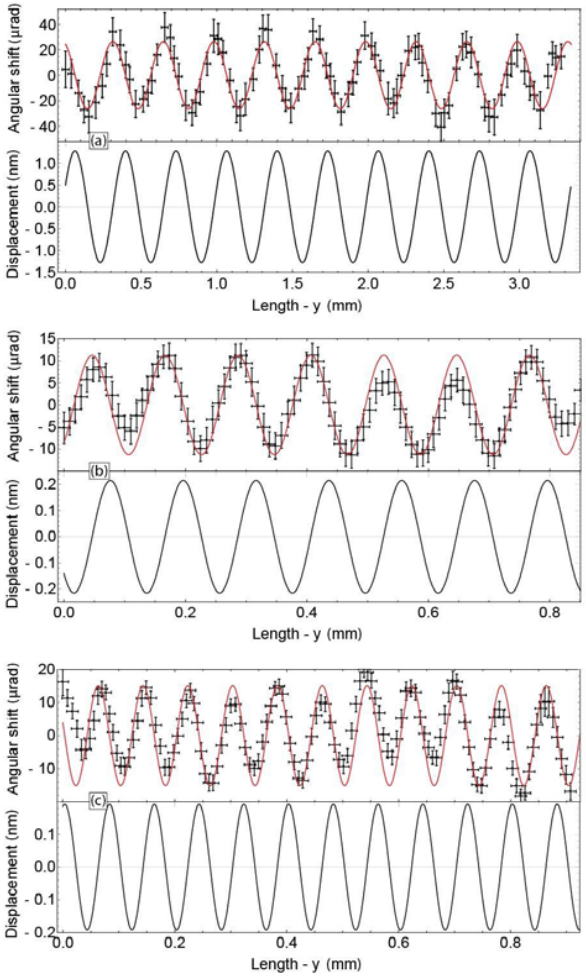

- Rocking Curve Imaging method at BM05- ESRF (Diamond-Boron)

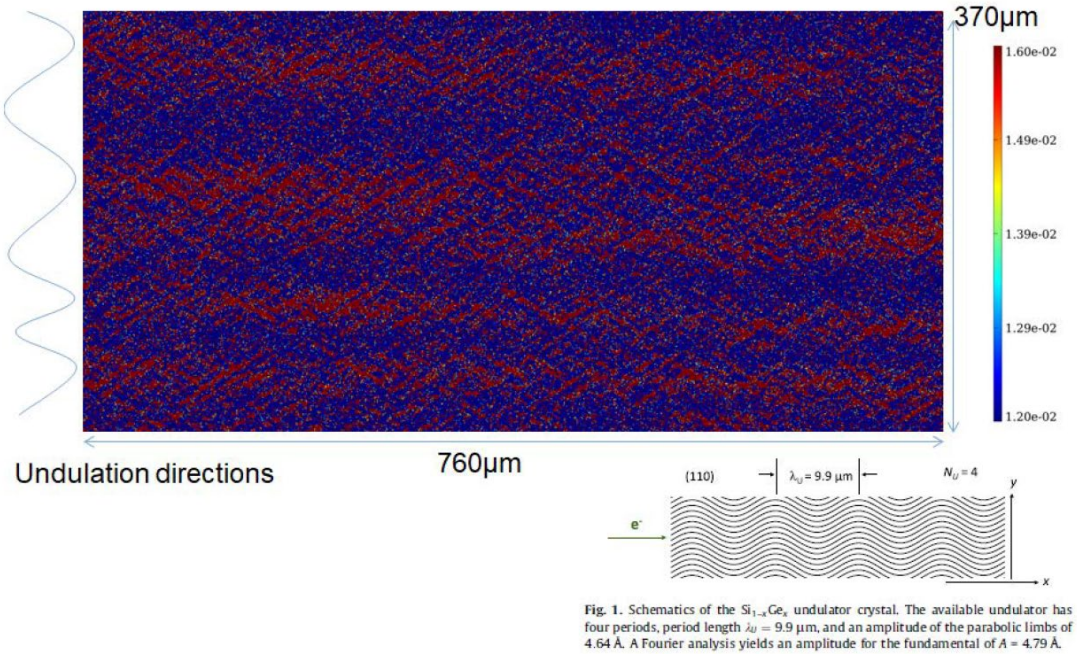

Fig. 1. Schematics of the $Si_{1-x}Ge_x$ undulator crystal. The available undulator has four periods, period length λ_U = 9.9 µm, and an amplitude of the parabolic limbs of 4.64 Å. A Fourier analysis yields an amplitude for the fundamental of A = 4.79 Å.

Figure 2.3: *RCI analysis:* FWHM map (in degrees) of $Si_{1-x}Ge_x$. Image size is 0.76x0.37mm^2.

Thu Nhi Tran Thi, J. Morse, D. Caliste, B. Fernandez, D. Eon, J. Härtwig, et al. J. Appl. Cryst. 50 (2017) 561-569.

R. Camattari, L. Bandiera, *et al,* Phys. Rev. Accel. Beams **22**, 044701 (2019)

Experiments at the DIAMOND Light Facility

MBN Research Center

Examples of crystal channellers: 15 µm bent Si

15 µm thick bent Si crystal
Nominal radius: 3 cm

Peak: range
0.702-0.847 deg

Peak: range
0-0.850 deg

16 mm

- 15 keV X-rays from Si (111) double-crystal mono
- Contour plots showing pixel-by-pixel variation of peak angle over rocking curve:
- Varying width of bright region with height indicates non-uniform curvature.
- Slant of bright region from top to bottom indicates torsion.

diamond

Optics and Metrology

Slide the presentation by J. Sutter at the ISACC 2023, July 20-22, 2023 Iceland
Joint experiment with TECNO-CLS UNIFE and INFN teams.

MBN
Research Center

MBN Explorer and MBN Studio 5.0: recent implementations and TECHNO-CLS related case studies

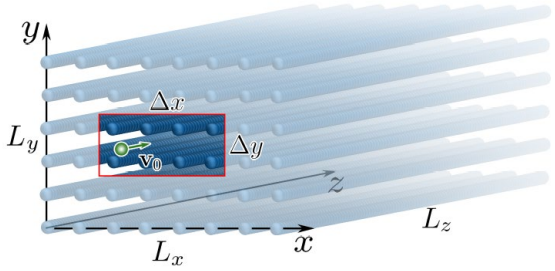

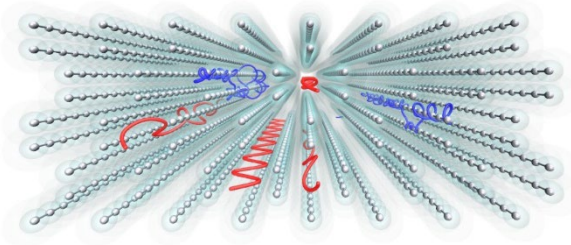

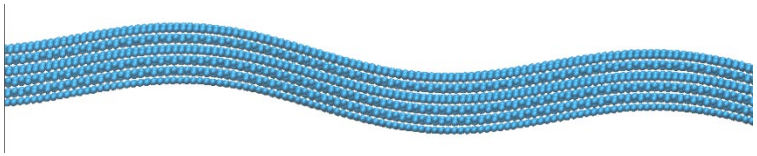

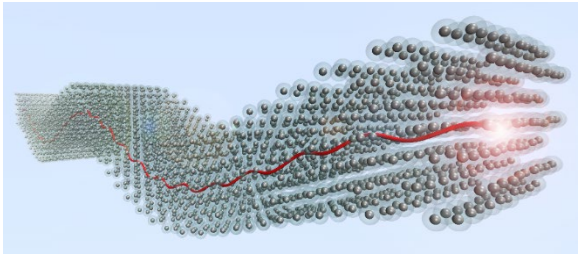

MBN (MesoBioNano) Explorer 5.0

MBN Research Center

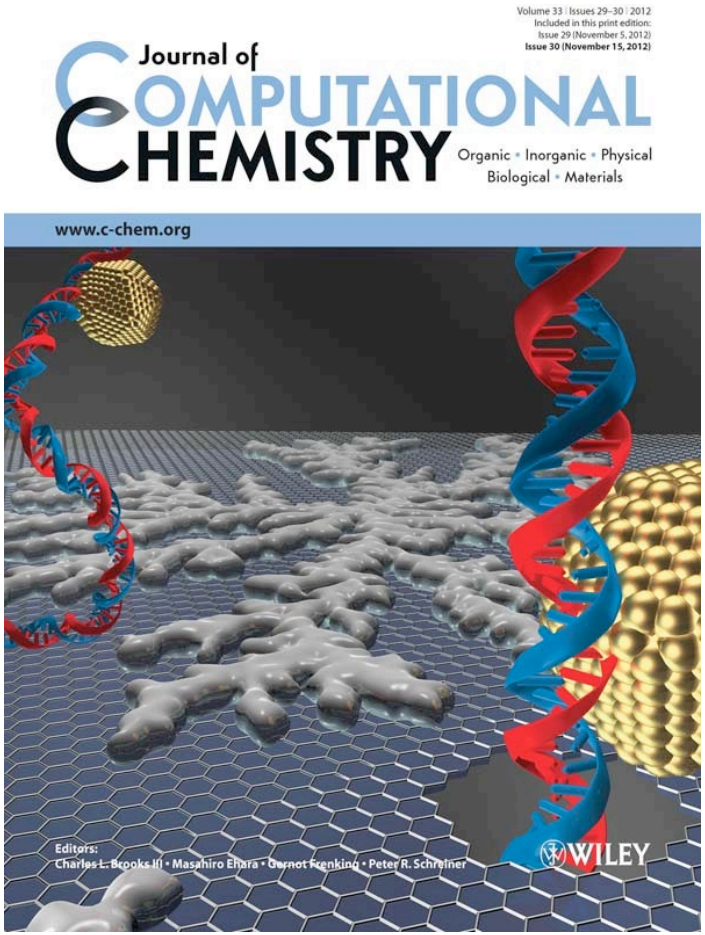

I.A. Solov'yov, A.V. Yakubovich, P.V. Nikolaev, I.Volkovets, and A.V. Solov'yov, *Meso Bio Nano Explorer -- a universal program for multiscale computer simulations of complex molecular structure and dynamics*. Journal of Computational Chemistry, volume 33, pp. 2412-2439 (2012) & **volume cover**.

MBN (MesoBioNano) Explorer is a powerful software package for multiscale simulations and visualisation of complex molecular structure and dynamics. It has many unique features, a wide range of applications in Physics, Chemistry, Biology and Material Science, and related Industries.

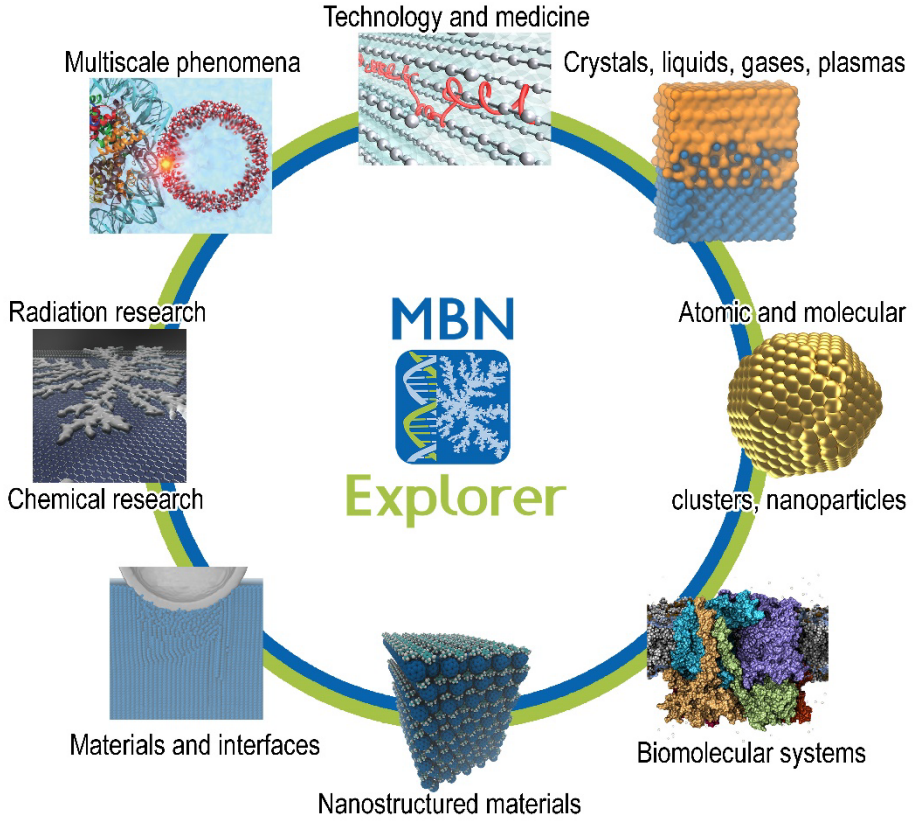

MBN Explorer is being developed by the MBN Research Center www.mbnresearch.com in Frankfurt.

MBN Explorer and MBN Studio books

MBN Research Center

MBN Explorer: relativistic dynamics

MBN Research Center

Simulation of motion of relativistic particles in MBN Explorer is based on relativistic equations of motion.

$$\begin{cases} \dot{\mathbf{v}} = \dfrac{1}{m\gamma}\left(\mathbf{F} - \mathbf{v}\dfrac{(\mathbf{F}\cdot\mathbf{v})}{c^2}\right) \\ \dot{\mathbf{r}} = \mathbf{v} \end{cases}$$

This system of equations is strongly nonlinear and requires the use of high-order integrator in order to be solved correctly.

$$\gamma = \frac{1}{\sqrt{1 - v^2/c^2}} \, .$$

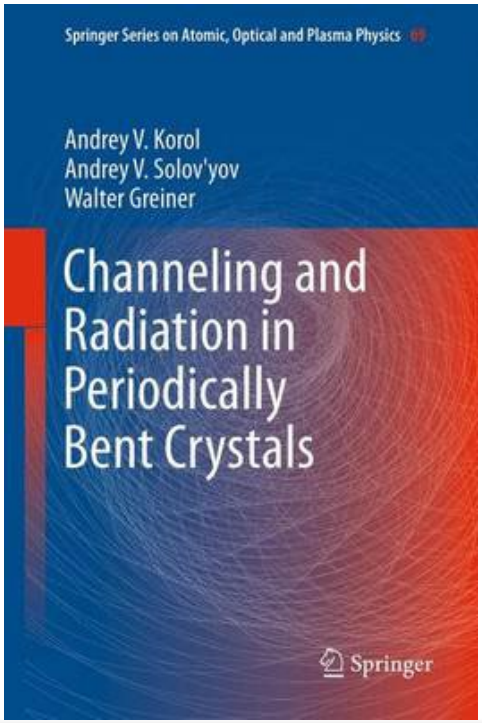

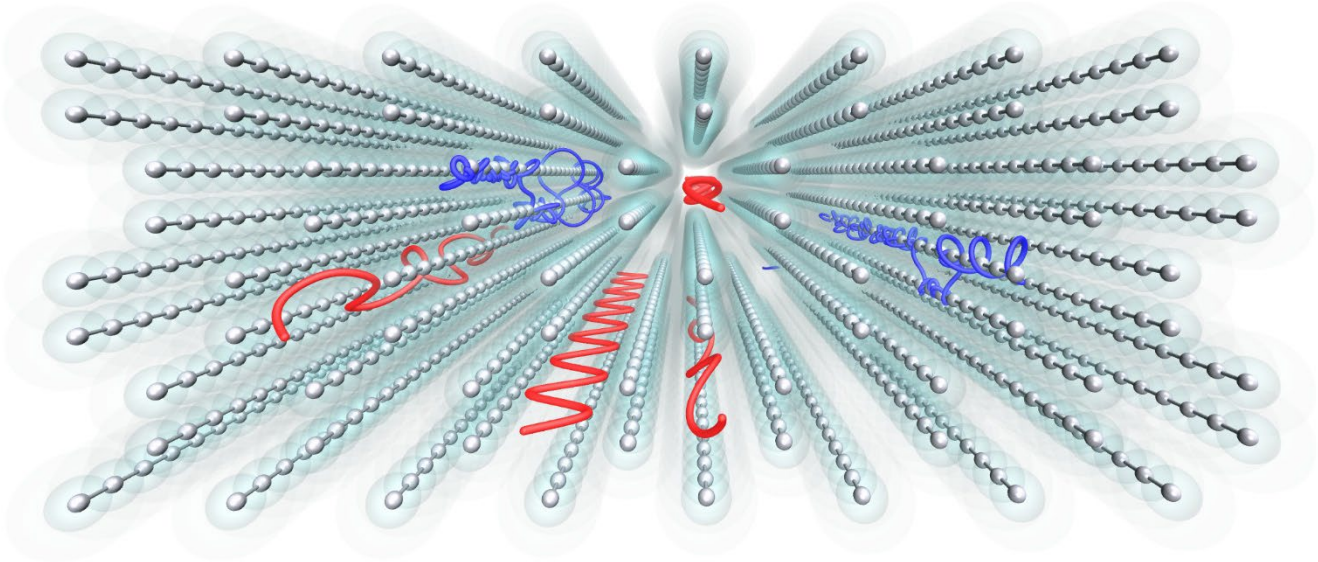

The developed approach (G.B. Sushko, V.G. Bezchastnov, I.A. Solov'yov, A.V. Korol, W. Greiner, A.V. Solov'yov, Journal of Computational Physics, 252, 404 (2013) is not restricted to the crystalline medium and is applicable to describe the propagation of ultra-relativistic projectile in an arbitrary medium.

Electron vs positron simulations

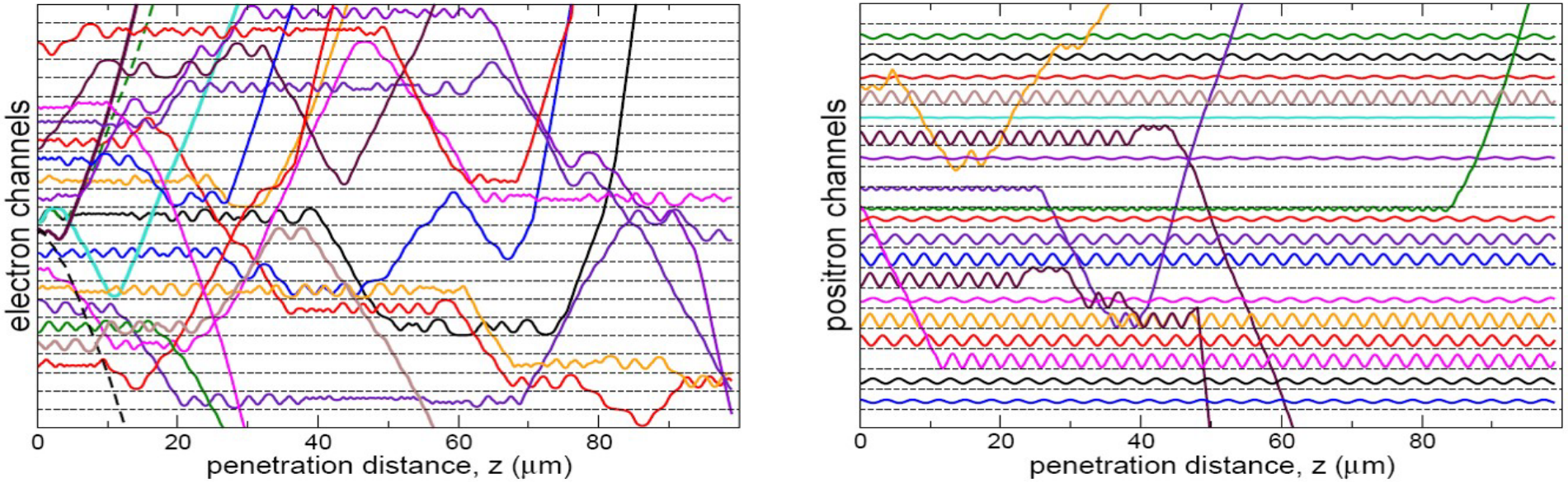

Channeling of 855 MeV electrons (left panel) and positrons (right panel) in a 100μm thick Si crystal. The plots show randomly chosen trajectories of the particles initially collimated along Si(111). Horizontal lines indicate the (111) planar channels.

G.B. Sushko, A.V. Korol, W. Greiner, A.V. Solov'yov, J. Phys.: Conf. Ser. 438, 012018 (2013)

Calculated characteristics

MBN Research Center

Simulated trajectories are analyzed further to calculate/estimate:

- Acceptance: $\mathcal{A} = \dfrac{N_{\mathrm{acc}}}{N_0}$

- Fractions of channeling particles: $\begin{cases} \xi_{\mathrm{ch0}}(z) = \dfrac{N_{\mathrm{ch0}}(z)}{N_0} \\ \xi_{\mathrm{ch}}(z) = \dfrac{N_{\mathrm{ch}}(z)}{N_0} \end{cases}$

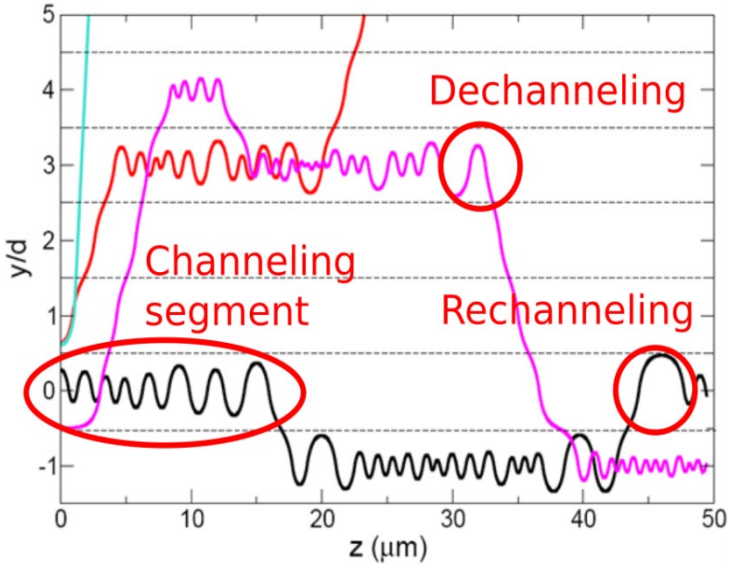

- Dechanneling length: $N_{\mathrm{ch}}(z) \propto N_0 \exp\left(-z/L_{\mathrm{d}}\right)$

- Distribution in the deflection angle

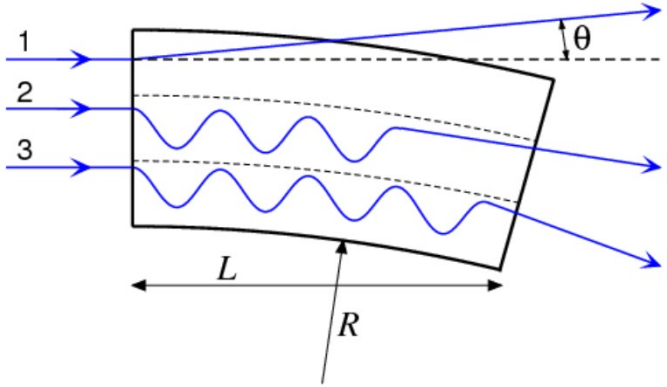

Spectral and angular distribution of emitted radiation: theory vs exp

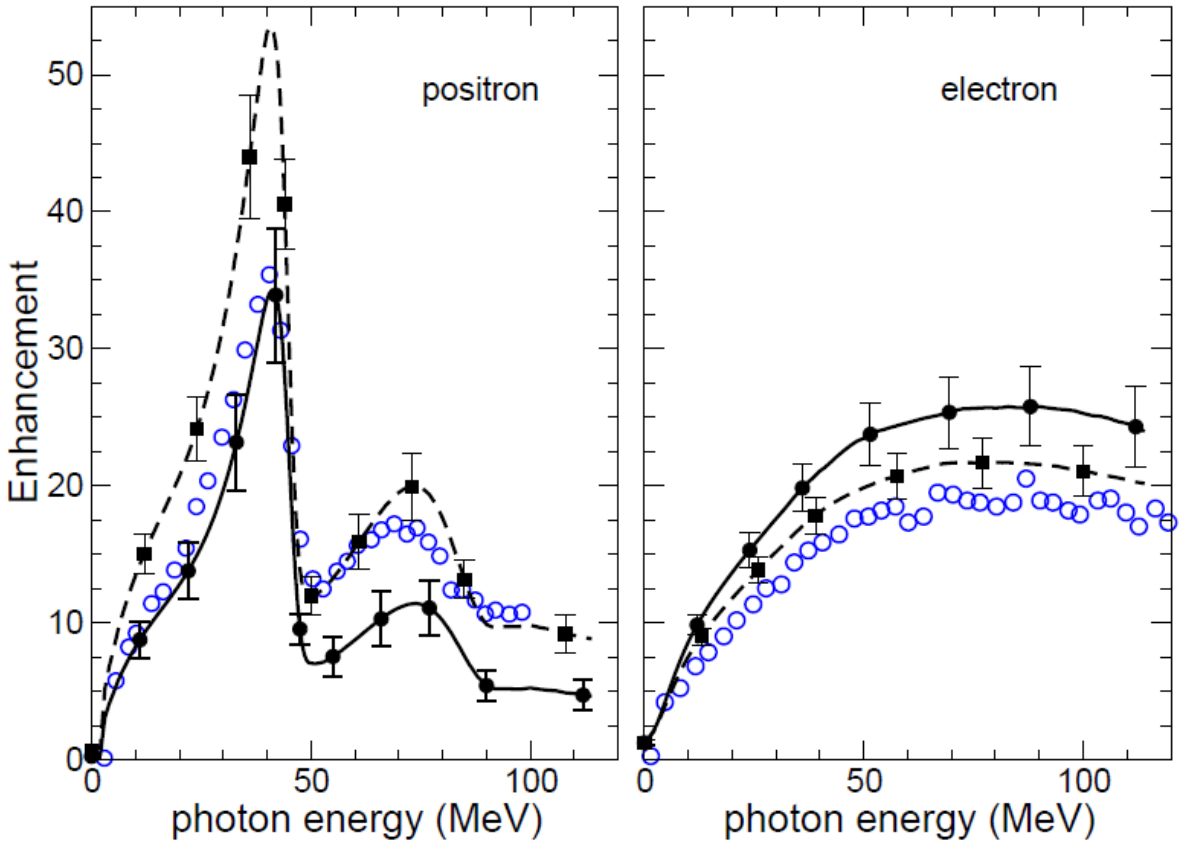

Figure 6: Enhancement factor of the channeling radiation over the Bethe-Heitler spectrum. The left and right plots are for the positrons and electrons, respectively. Open circles stand for the experimental data [31]. Solid curves correspond to the calculations shown in Fig. 5 and correspond to the zero incident angle, $\psi = 0$. Dashed curves correspond to the calculations with the incident angle lying within $\psi = [-\psi_L, \psi_L]$ with $\psi_L = 62$ μrad. See also explanation in the text.

Comparison of experimentally measured channeling radiation enhancement
(J. Bak, J.A. Ellison, E.Uggerhoj et al (1985))

with theoretical results
(G.B. Sushko, V.G. Bezchastnov, I.A. Solov'yov, A.V. Korol, W. Greiner, A.V. Solov'yov, Journal of Computational Physics, v.252, p.404–418 (2013))

for 6.7 GeV positrons and electrons in Si(110)

$$\text{Enhancement} = \frac{\mathrm{d}E_{\text{Si(110)}}}{\mathrm{d}E_{\text{am}}}$$

Advances and challenges in atomistic approach for relativistic MD

➢ Accounting for ionizing collisions

Inelastic scattering from target electrons results in the following instant changes:

(1) Random change in the projectile energy, $\Delta\varepsilon < 0$.

(2) Random change in the direction of the projectile motion characterized by two scattering angles θ and φ measured with respect to the instant velocity.

At each step of integration of EM the collisions are treated as probabilistic events. Once the event occurs and the value $\Delta\varepsilon$ is found, the scattering angles are determined leading to the instant change in the velocity of a projectile.

➢ Radiation damping

A charged particle moving in a medium looses its energy due to the emission of electromagnetic radiation. The emission gives rise to a *radiative reaction force f* acting on a projectile. Its action leads to the radiation damping, i.e. to a gradual decrease of the particle's energy. For ultra-relativistic projectiles of high energies (tens of GeV and above) this force becomes quite noticeable so that it must be accounted when simulating the motion.

$$\mathbf{f} = \frac{2e^3}{3mc^3}\left(\gamma(\mathbf{v}\cdot\nabla)\mathbf{E} + \frac{e}{mc}(\beta\cdot\mathbf{E})\mathbf{E} - \gamma^2\frac{e}{mc}\left[\mathbf{E}^2 - (\beta\cdot\mathbf{E})^2\right]\beta\right)$$

Advances and challenges in atomistic approach for relativistic MD

MBN Research Center

➢ Account for beam emittance

Beam particles are distributed in the transverse coordinates (x,y) and velocities. The latter define the angular divergence, $\varphi_{x,y}$, of the beam. Two types of distributions are implemented:
(1) uniform distributions within specified intervals,
(2) normal (Gaussian) distributions with specified standard deviation σ:

$$f(\xi) = \frac{1}{\sqrt{2\pi\sigma^2}} \exp\left(-\frac{\xi^2}{2\sigma^2}\right) \quad \text{where} \quad \xi = (x, y, \phi_x, \phi_y)$$

➢ Modelling quasi-mosaic bent crystals (qmBC)

qmBCs belong to a class of bent crystals featuring three curvatures of two orthogonal crystallographic planes.

As a crystal is bent to a primary curvature by external forces, a secondary curvature is generated within the crystal, i.e. the quasi-mosaic curvature.

The planes bent by the QM effect are orthogonal to the main surface of the plate.

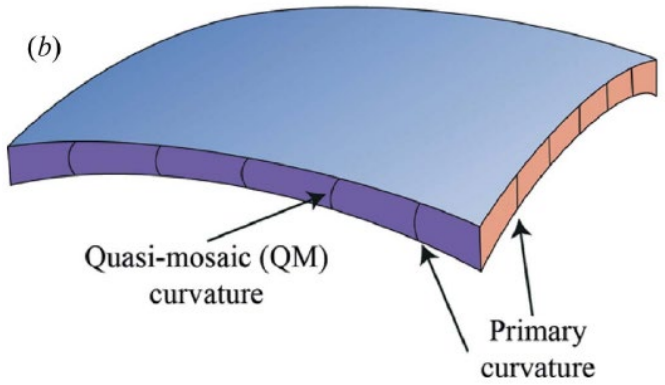

Schematic representation of a deformed plate with 'quasi-mosaic' curvature. Figure from R.Camattari et al. *J. Appl. Cryst.* 48, 977 (2015).

➢ Irradiation-induced damage of the target material

Advances and challenges in atomistic approach for relativistic MD

MBN Research Center

➢ Irradiation-induced damage

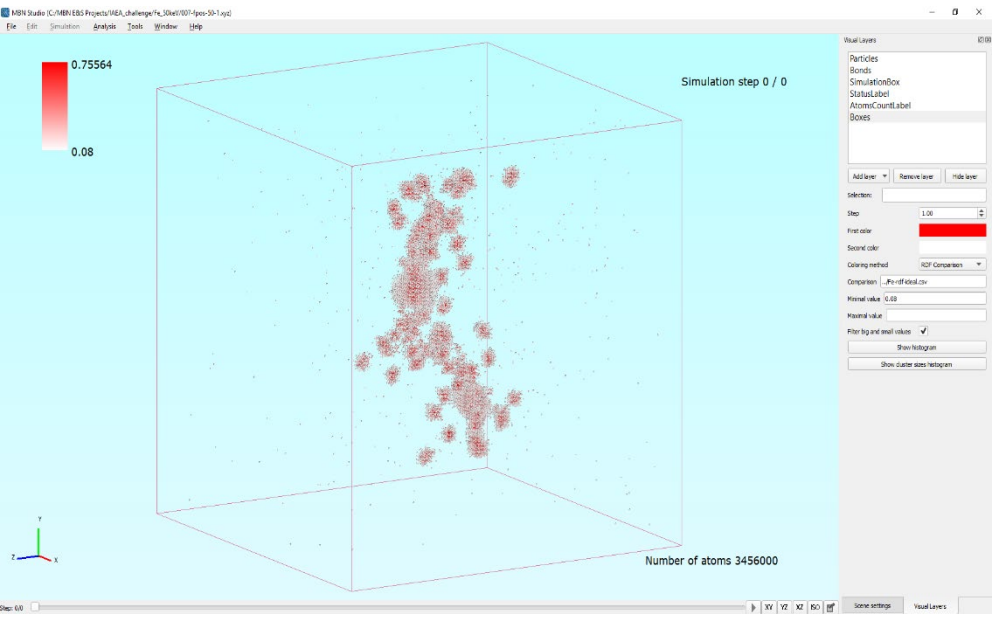

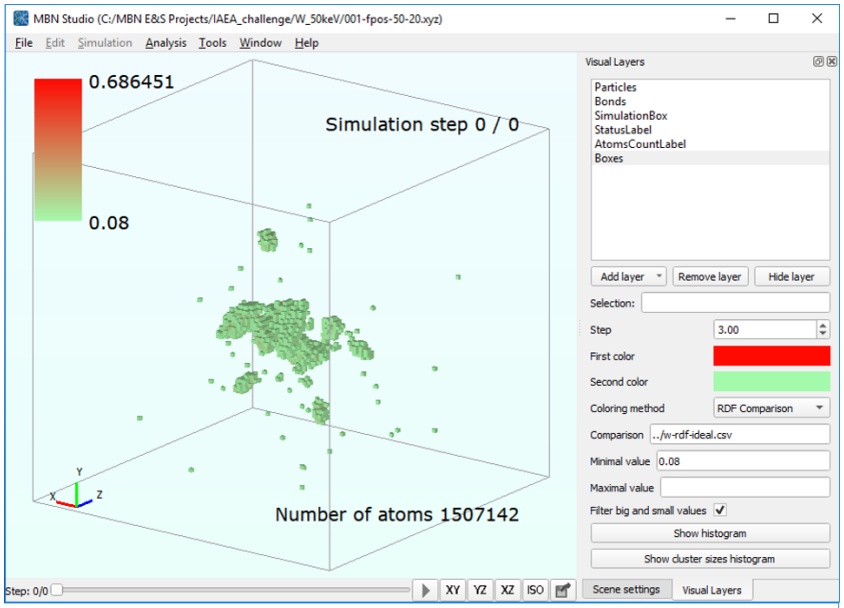

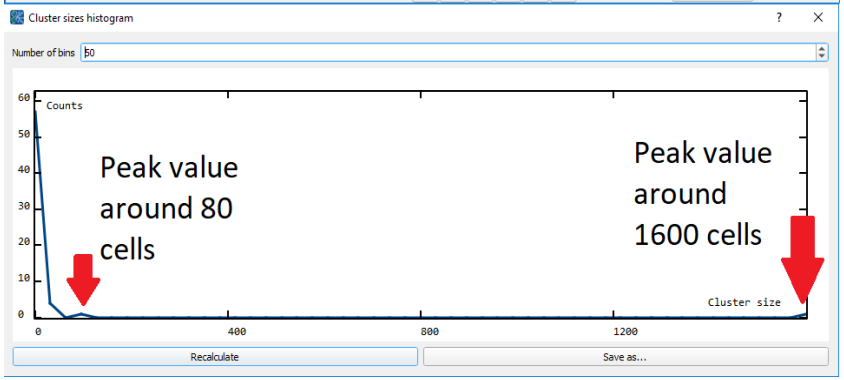

TECHNO-CLS collaborative work

MBN Research Center

- ***Atomistic simulations of CLSs and related phenomena with MBN Explorer***
  - Andrei Korol, A.V. Solov'yov (MBN RC)
  - Matthew Dickers, Klaudia Cielinska, Nigel Mason (UoK)
- ***Manufacture and characterisation of linear, bent and periodically bent crystal structures***
  - Coactive patterning: Andrea Mazzolari (INFN)
  - Pulsed laser melting: Davide De Salvador (UNIPD)
  - Acoustical excitation: Konstantinos Kaleris (HMU)
  - Boron-doped diamond: Thu Nhi TRAN CALISTE (ESRF)

Crystal-based gamma-ray LS (CLS)

MBN Research Center

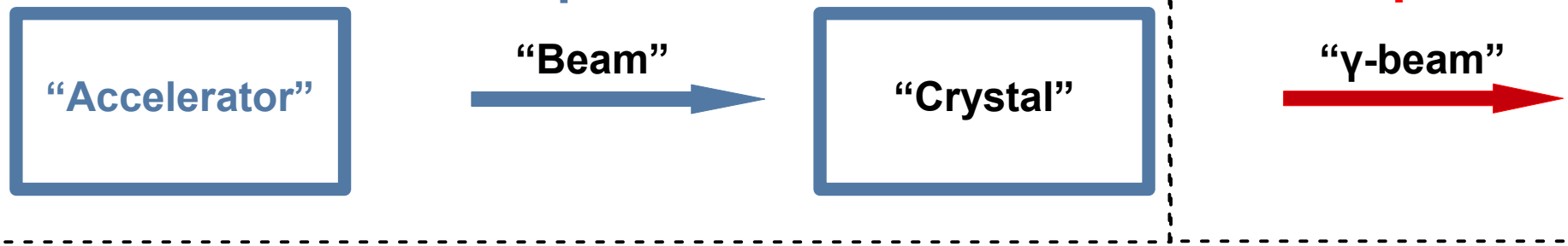

Principal elements:
- Type of accelerator
- Apparatus
- Beam line
- Infrastructure

Characterisation of the beam:
- Type of projectile
- Energy and energy spread
- Size
- Emittance
- Current

Relevant issues:
- Crystal manufacture;
- Structure characterisation
- Crystal manipulation
- Channeling experiments
- Advanced simulations

Experimental and theoretical characterisation of radiation:
- Spectral-angular distribution
- Number of photons
- Brilliance
- Power

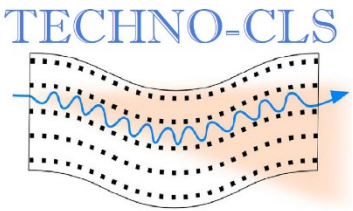

Superradiant CUR versus FEL and SR

MBN Research Center

Brilliance of a photon source relates the number of photons of a given energy emitted per unit time interval, unit source area, unit solid angle and per bandwidth:

$$B_n = \frac{\Delta N_{\omega_n}}{10^3 \left(\Delta\omega_n/\omega_n\right)(2\pi)^2 \varepsilon_x \varepsilon_y} \frac{I}{e}$$

- n – harmonic number
- $\omega_n, \Delta\omega_n$ – energy and width of the nth harmonic
- $\Delta\omega_n/\omega_n$ – bandwidth (=BW)
- ΔN_{ω_n} – number of photons with $\omega \in \left[\omega_n - \Delta\omega_n/2, \omega_n + \Delta\omega_n/2\right]$
- I – electric current of the beam
- $\varepsilon_{x,y}$ – emittance of the photon source along

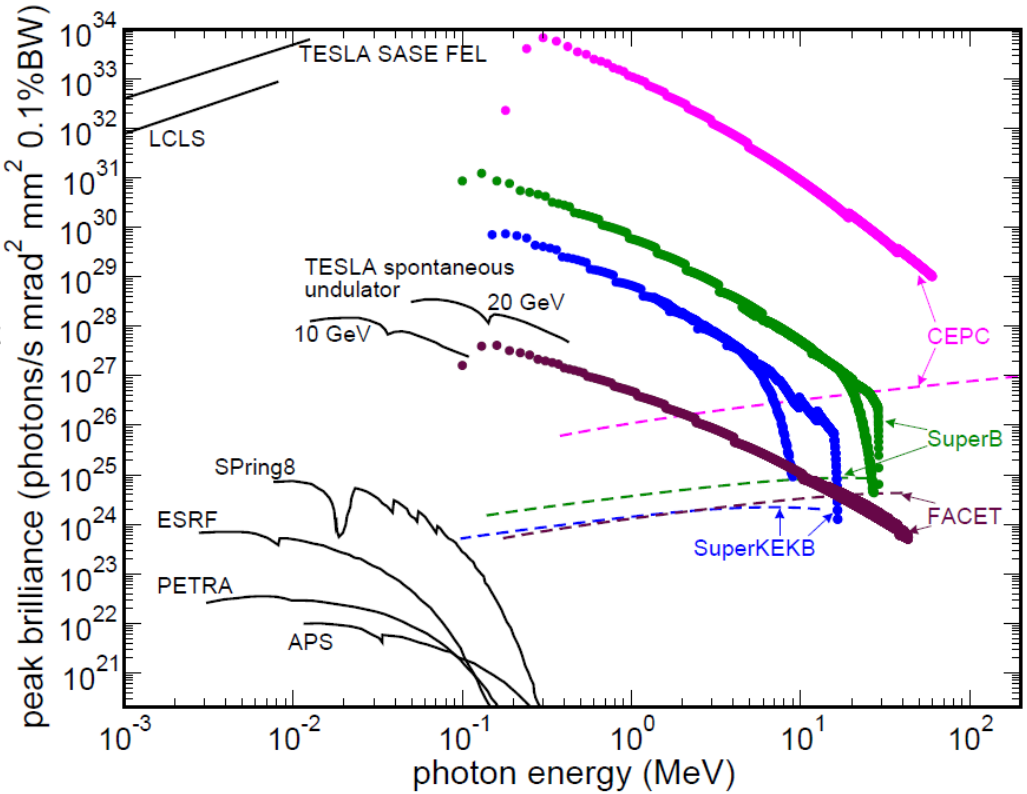

Figure 5. Peak brilliance of superradiant CUR (thick solid curves) and spontaneous CUR (dashed lines) from diamond(110) CUs calculated for the SuperKEKB, SuperB, FACET-II and CEPC positron beams versus modern synchrotrons, undulators and XFELs.

A.V Korol, A.V Solov'yov, *Crystal-based intensive gamma-ray light sources (Topical Review)*, Eur. Phys. J. D (2020) 74: 201

Recent exemplar case studies: CU-LS

MBN Research Center

Simulations are performed for 10 GeV positron beam available at present at the SLAC facility

TABLE II. Two sets of parameters of diamond-based CUs used in the simulations: bending amplitude a, period λ_u, number of periods N_u, crystal thickness $L = N_u\lambda_u$. The last column presents the energies $\hbar\omega_0$ of the fundamental harmonic in the forward direction.

Set	a (Å)	λ_u (μm)	N_u	L (mm)	$\hbar\omega_0$ (MeV)
(I)	20.9	85	85	7.06	2.0
(II)	5.3	38	180	6.84	10.0

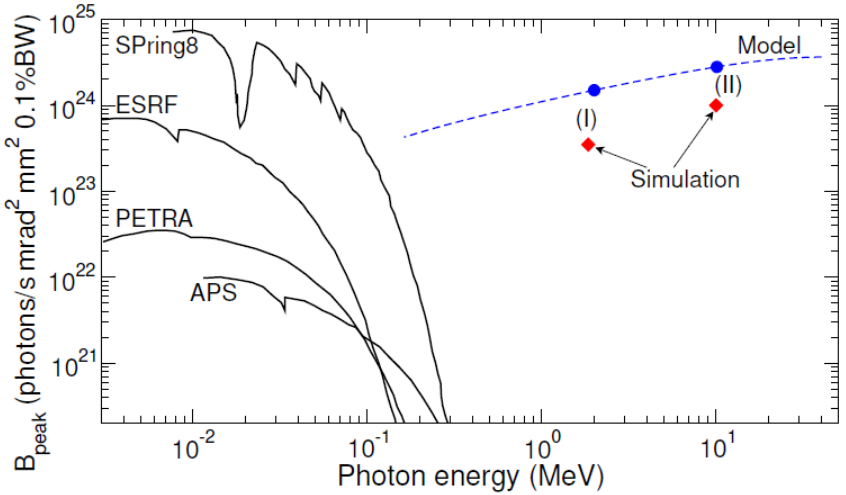

FIG. 5. Comparison of the peak brilliance available at several synchrotron radiation facilities (APS, ESRF, PETRA, SPring8) with that for the CU-LS. The filled diamond symbols show the brilliances that correspond to Sets (I) and (II) in Table II. The dashed line stands for the model estimation [1]; the filled circles marked the estimated brilliances for Sets (I) and (II).

G.B. Sushko, A.V. Korol and A.V. Solov'yov, ***Extremely brilliant crystal-based light sources***, Eur. Phys. J. D, Eur. Phys. J. D, **76** (2022) 166

Conclusions and outlook

EIC TECHNO-CLS research directions

MBN Research Center

- Atomistic level simulations of particle propagation and photon emission in oriented crystals (linear, bent, PBBs, etc) with a predictive power
- Advances in technologies for manufacturing HQ crystals with desired properties (periodicity, composition, quality, size, etc)
- Experiments with high energy and quality electrons **and positrons** beams on verification of theoretical predictions
- Design, construction and characterisation of oriented crystal based light sources with unique properties
- An utmost goal: adopting FEL principles to CU-based Superradiant light sources operating with modulated beams of electrons and positrons
- Growing international community in the R&D area of oriented crystal based light sources and their practical realisation

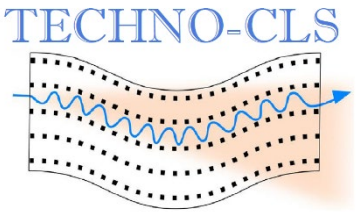

MBN Explorer and MBN Studio 5.0

MBN Research Center

- **MBN Explorer & Studio software 5.0** are the powerful instruments for advanced theoretical and computational research and **multiscale modelling** of structure and dynamics of complex Meso-Bio-Nano (MBN) systems.
- **MBN Explorer & Studio software** can be utilised for teaching of many disciplines
- **MBN Explorer & Studio** are being developed by the **MBN Research Center** in Frankfurt, www.mbnresearch.com. **You are welcome to contact us!**

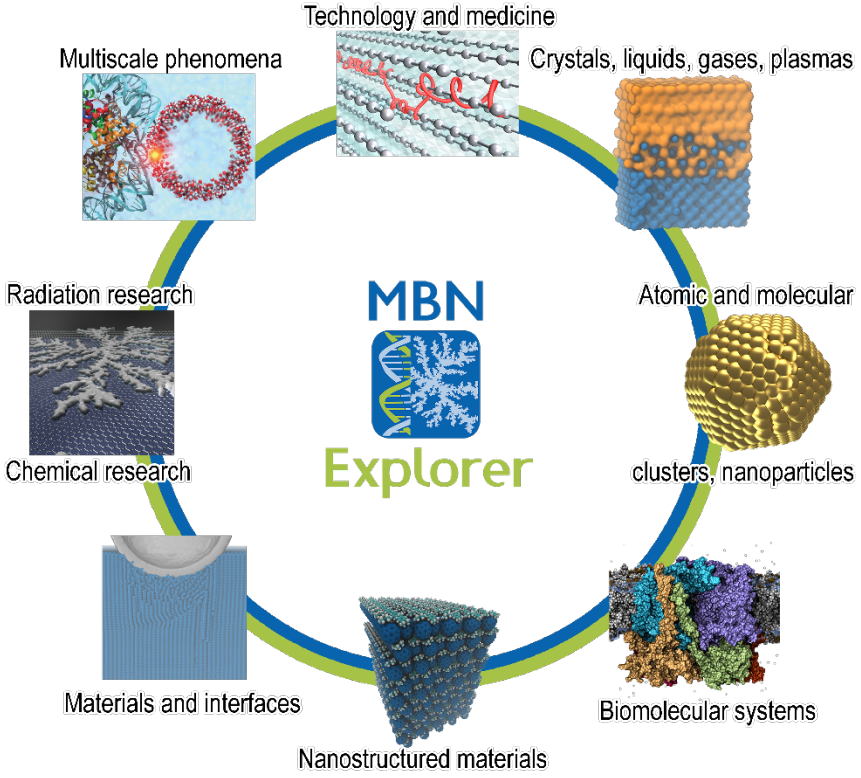

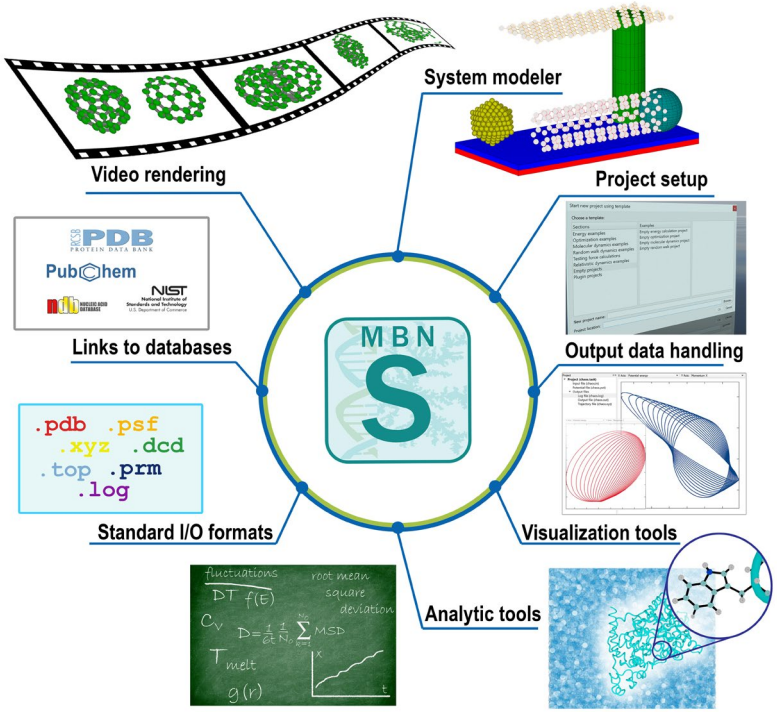

Acknowledgements to the team

MBN Research Center

Members and visitors:

- Andrei Korol
- Ilia Solov'yov
- Irina Solovyeva
- Gennady Sushko
- Alexey Verkhovtsev
- Alexey Prosvetov
- Matthew Dickers
- Klaudia Cielinska


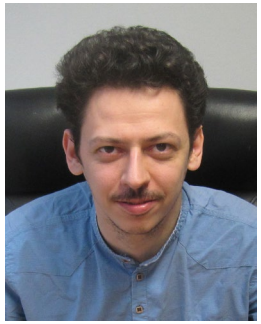
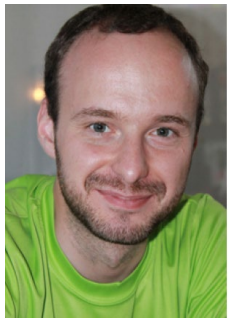





Former members & visitors: Viktor Beschastnov, Pablo de Vera, Yury Erofeev, Yannick Fortouna, Viktar Haurylavets, Vadim Ivanov, Sergey Kazenyuk, Christian Kexel, Andrey Lyalin, Pavel Nikolaev, Oleg Obolensky, Mikhail Panshenskov, Roman Polozkov, Alexander Pavlov, Veronika Dick/Semenikhina, Eugene Surdutovich, Ilya Volkovetz, Alexander Yakubovich

Current EU projects Consortia: H2020 RISE-RADON, H2020 RISE-N-LIGHT, COST Action MultIChem, EIC Pathfinder Project TECHNO-CLS

Thank you for your attention !